

Article

Tectonic Control, Reconstruction and Preservation of the Tiegelongnan Porphyry and Epithermal Overprinting Cu (Au) Deposit, Central Tibet, China

Yang Song ^{1,*}, Chao Yang ², Shaogang Wei ³, Huanhuan Yang ^{1,4}, Xiang Fang ^{1,2} and Hongtao Lu ¹

¹ Key Laboratory of Metallogeny and Mineral Assessment, Institute of Mineral Resources, Chinese Academy of Geological Sciences, Beijing 100037, China; zggyhh@163.com (H.Y.); francisfx@126.com (X.F.); hai5987@163.com (H.L.)

² Department of Geology and Geological Engineering, University Laval, QC G1V 0A6, Canada; yangchao2012cags@126.com

³ First Crust Monitoring and Application Center, China Earthquake Administration, Tianjin 300180, China; shaogang_wei@yahoo.com

⁴ College of Earth, Ocean, and Atmospheric Sciences, Oregon State University, Corvallis, OR 97331, USA

* Correspondence: songyang@mail.cgs.gov.cn; Tel.: +86-010-6899-9087

Received: 9 May 2018; Accepted: 6 September 2018; Published: 10 September 2018



Abstract: The newly discovered Tiegelongnan Cu (Au) deposit is a giant porphyry deposit overprinted by a high-sulfidation epithermal deposit in the western part of the Bangong–Nujiang metallogenic belt, Duolong district, central Tibet. It is mainly controlled by the tectonic movement of the Bangong–Nujiang Oceanic Plate (post-subduction extension). After the closure of the Bangong–Nujiang Ocean, porphyry intrusions emplaced at around 121 Ma in the Tiegelongnan area, which might be the result of continental crust thickening and the collision of Qiangtang and Lhasa terranes, based on the crustal radiogenic isotopic signature. Epithermal overprinting on porphyry alteration and mineralization is characterized by veins and fracture filling, and replacement textures between two episodes of alteration and sulfide minerals. Alunite and kaolinite replaced sericite, accompanied with covellite, digenite, enargite, and tennantite replacing chalcocite and bornite. This may result from extension after the Qiangtang–Lhasa collision from 116 to 112 Ma, according to the reopened quartz veins filled with later epithermal alteration minerals and sulfides. The Tiegelongnan deposit was preserved by the volcanism at ~110 Ma with volcanic rocks covering on the top before the orebody being fully weathered and eroded. The Tiegelongnan deposit was then probably partly dislocated to further west and deeper level by later structures. The widespread post-mineral volcanic rocks may conceal and preserve some unexposed deposits in this area. Thus, there is a great potential to explore porphyry and epithermal deposit in the Duolong district, and also in the entire Bangong–Nujiang metallogenic belt.

Keywords: tectonic control; overprinting; preservation; vein-filling; replacement; porphyry; epithermal; Tiegelongnan; Tibet

1. Introduction

In the past two decades, some large porphyry deposits have been found in Tibet, China, such as Yulong deposit (6.22 Mt at 0.99% Cu) [1], Qulong deposit (7.1 Mt at 0.5% Cu) [2], Jiama deposit (7.4 Mt at 0.5% Cu) [3], Duobuza deposit (2.9 Mt at 0.46% Cu) [4], and Bolong deposit (3.8 Mt at 0.5% Cu) [5]. This indicates that Tibet can be considered one of the most significant potential porphyry Cu systems in the world. Recently, epithermal deposits have also been discovered and reported in Tibet. Epithermal deposits are genetically associated with porphyry Cu deposits, especially high and

intermediate sulfidation epithermal ones, which could be discovered at upper or lateral locations of porphyry deposits in some cases [6]. However, the epithermal deposits do not always occur close to porphyry deposits, because epithermal deposits are normally at shallow crustal levels (surface to 1–2 km depth), therefore they could be easily eroded by later orogenesis [6].

The Duolong porphyry Cu-Au district is located in the Bangong–Nujiang metallogenic belt (BNMB), central Tibetan Plateau, which was discovered in 2007 and hosts several large porphyry and epithermal deposits and ore prospects (Figure 1). The Tiegelongnan deposit was discovered in 2013, containing the largest scale Cu resource within this district, and it was documented as a porphyry Cu (Au) deposit overprinted by high-sulfidation mineralization [7]. The total Cu content persevered in the Tiegelongnan deposit is around 1600 Mt at 0.51% Cu. The Au content is small at about 280 Mt with a low grade of 0.13g/t Au on average.

Despite numerous studies on the metallogeny of the Tiegelongnan deposit, the tectonic control of this type deposit has rarely been demonstrated. Formation of the porphyry and epithermal deposits in the Duolong district was indicated to be associated with the magma arising from the closure of the Bangong–Nujiang Ocean (BNO) in the Early Cretaceous [8,9]. However, how the tectonic activities control the formation of the porphyry Cu system is controversial. The Tiegelongnan deposit is the first high-sulfidation epithermal deposit being discovered in the Tibetan Plateau. Previous studies suggested that the limited number of epithermal deposits found in the Tibetan Plateau is due to the dramatic uplift and deep level erosion. The Tiegelongnan deposit is an example to study the tectonic control, reconstruction and preservation process of porphyry Cu systems in the Tibetan Plateau. In this study, we reviewed history of the tectonic setting, magma emplacement, multiple episodes' mineralization, exhumation, and preservation of the Tiegelongan deposit, based on published literatures and the detailed drill core logging and deposit 1:500 scale mapping. Besides, we discussed the implications of this study on exploration of porphyry and epithermal deposits in the Duolong district and other places in Tibet.

2. The Duolong District

The Duolong ore district is located approximately at 100 km northwest of Gerze county, on the western BNMB (Figure 1). This belt is supposed to be a suture zone as the remnants of the Bangong–Nujiang Ocean (BNO) which records the evolution of the BNO during the period of Permian to Cretaceous. This belt is over 2000 km-long striking to the east, and it is dominated by Jurassic–Cretaceous flysch, mélange, and ophiolitic fragments [10,11]. The Bangong–Nujiang suture zone extends across the central Tibetan Plateau, which separates the Qiangtang and Lhasa terranes (Figure 1a) [12,13].

There are several porphyry deposits, epithermal deposits, and porphyry and epithermal ore prospects in the Duolong district (Figure 1). The Duobuza [4], the Bolong [5], and the Naruo [14] are porphyry Cu (Au) deposits. Whereas, the Tiegelongnan deposit is a porphyry deposit overprinted by epithermal deposit [7,15]. In the Dibao, Nadun, Sena, Saijiao, and the Ga'erqin areas, there are porphyry or epithermal ore prospects (Figure 1b). Li et al., (2011) and Lin et al., (2017) suggested these deposits are related to granodiorite and quartz diorite porphyry intrusions being emplaced during 123–116 Ma, and their mineralization timing is between 120 Ma and 118 Ma [16,17].

The intrusions in the Duolong district are dominated by intermediate to felsic rocks with minor gabbro. The granodiorite porphyry and quartz-diorite porphyry are more widespread than other rock types—including diorite, granodiorite, and gabbro. The porphyry and epithermal deposits in the Duolong district are hosted by the granodiorite and quartz diorite porphyries, and also by the contact zone between these intrusions and the Jurassic quartz-feldspar sandstones. Volcanic rocks like basalt, andesite, and basaltic andesite are also widespread in the Duolong district. These volcanic rocks in this district all belong to the Meiriqiecuo Formation (K_1m) unconformably overlying on the sedimentary rocks.

The sedimentary sequences in the Duolong ore district are dominated by Mesozoic pelagic sediments and Cenozoic continental sediments including conglomerates and sandstones. These sequences are composed of the Upper Triassic Riganpeicuo Formation (T_3r), the Lower Jurassic Quse Formation (J_1q), the Lower to Middle Jurassic Sewa Formation ($J_{1-2}s$), the Upper Cretaceous Abushan Formation (K_2a), and the Upper Oligocene Kangtuo Formation (E_3k). The Riganpeicuo Formation dominated by limestone is unconformably overlain by the Quse and Sewa formations. The Quse Formation mainly occurred in the center and southwestern part of the ore district as the main host formation of the Duobuza and Bolong porphyry deposits. It conformably contacts with the overlying Sewa Formation, which is the predominant host formation of the Tiegelongnan deposit. These two Jurassic formations are thought to be part of the metamorphosed accretionary complex formed by north-dipping subduction of the BNO plate under the Qiangtang terrane [18]. They were also interpreted to be bathyal to abyssal flysch succession, implying a stable shallow-marine continental-shelf sedimentary environment along the southern continental margin of the South Qiangtang terrane [10]. Furthermore, Wei et al. (2017) [9] proposed that a continental margin arc setting in the southern Qiangtang terrane during the Early Cretaceous.

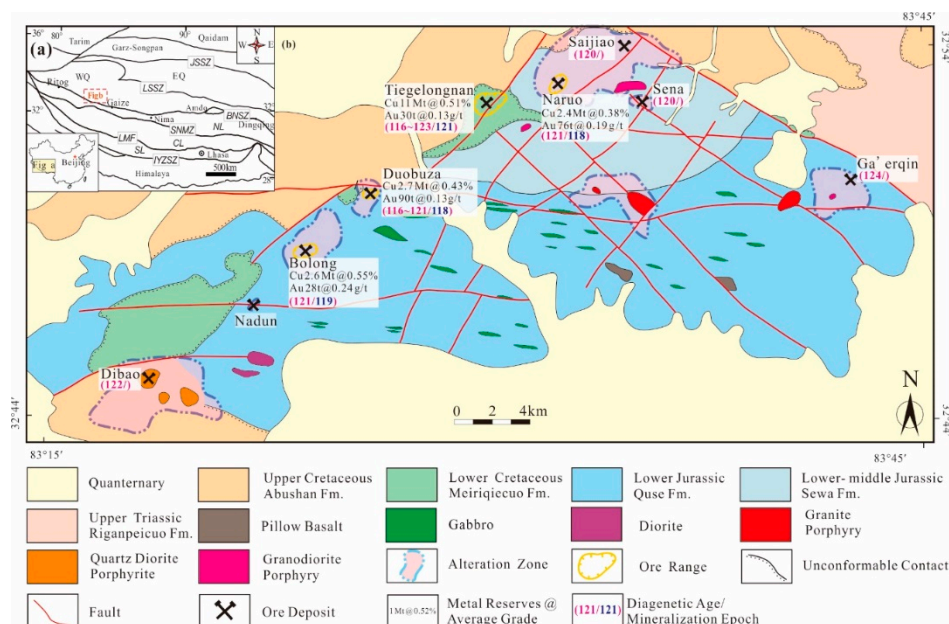


Figure 1. Regional geological map of the Duolong ore cluster, modified after [8], ages are from [17].

There are three main faults in the Duolong district striking at NE–SW, E–W, and NW–SE, respectively (Figure 1). The NE–SW fault is a major ore-controlling structure. A number of ore-bearing granodioritic porphyry intrusions emplaced along this fault, and therefore, many large porphyry copper deposits such as the Bolong, Duobuza, Tiegelongnan, and Naruo deposits occurred.

Most E–W thrust faults are large scale and traverse across the entire Duolong district, dipping to the south with an angle between 49° and 16° [19]. There are some granodiorite porphyries (125–120 Ma, unpublished data) beaded along this NE–SW fault. A mylonite sample obtained from the fault zone was well constrained with a $^{40}\text{Ar}/^{39}\text{Ar}$ plateau age at 127.8 ± 1.1 Ma [19], which represents an early period of thrusting. The NW–SE faults are normal slip faults dipping to the south, which might be related to the neo-tectonic movements. These faults are characterized by sunken landform and valleys with fault breccia exposed.

3. Tiegelongnan Alteration and Mineralization

The Tiegelongnan deposit is hosted by the Sewa Formation quartz-feldspar sandstones and some intermediate and felsic porphyry intrusions. These rocks were mostly concealed by the andesite of

the Meiriqiecuo Formation which is currently well exposed (Figure 2a). The earliest diorite porphyry within this deposit was intruded at 123 Ma before the mineralization, which is mainly distributed at the eastern and southern margins of this area [8]. Several phases of granodiorite porphyries are syn-mineral intrusions with ages ranging from 121 Ma to 116 Ma [8,20,21]. They are indistinguishable from petrology and crosscutting relationships, because subsequent strong alteration weakened their differences and boundaries. Therefore, the geochemistry data, especially the mobile elements, could not be used to discriminate their geochemical features.

3.1. Alteration

Drill core logging reveals concealed features of the Tiegelongnan deposit (Figure 2b). Five phases of hydrothermal alteration were identified in the Tiegelongnan deposit, according to the dominant alteration mineral assemblage, including: biotite alteration, sericite-pyrite-quartz (phyllitic) alteration, chlorite alteration, alunite alteration, and kaolinite-dickite alteration [22]. Alunite-kaolinite-dickite assemblages are also named as advanced argillic alteration in high-sulfidation epithermal deposits [23].

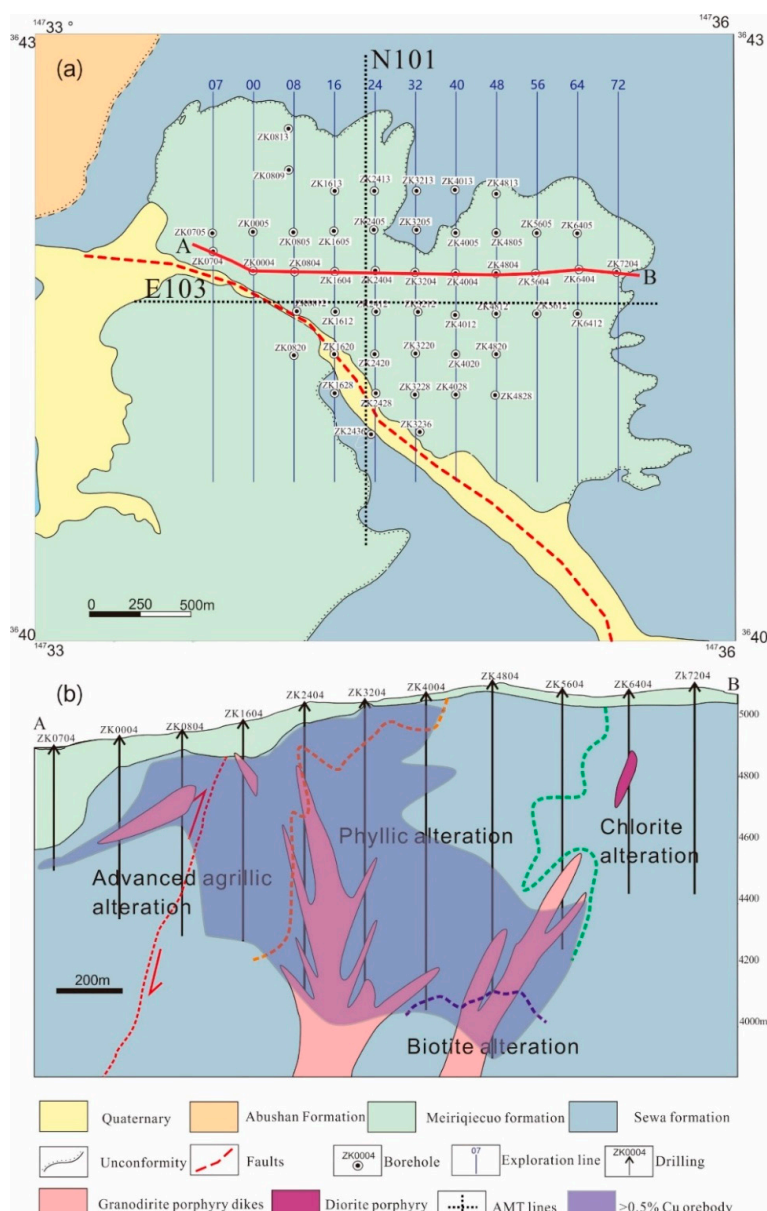


Figure 2. Ground surface and cross-section map of the Tiegelongnan porphyry Cu (Au) deposit.

Hydrothermal biotite occurs in wall-rock sandstones beneath an elevation of ~4100 m as disseminated fine grains and less commonly as vein biotite-quartz. It is not typical potassic alteration with no K-feldspar, and rare magnetite, rutile, and anhydrite. Sericite-pyrite-quartz (phyllitic) alteration is widespread in the Tiegelongnan deposit, hosting most of the ore minerals. These granodiorite porphyries and their surrounding sandstones are mostly altered to sericite and quartz. Some fluorite, rutile, anhydrite, and magnetite can be identified under the microscope. There are some quartz-chalcopyrite-pyrite and quartz-molybdenite veins occurring in the phyllitic alteration zone, not intensely. Chlorite alteration is in the southern and eastern part of the deposit, which scattered in the sandstone and diorite and pyrite-chlorite veins. Alunite mostly occurs in the alunite-sulfides veins, locally with kaolinite and dickite, distributed in a narrow and shallow place at a height ranging from 4500 m to 4950 m. Kaolinite-dickite alteration occurs as more widespread kao-dic veins than the alunite veins, which is featured with kaolinite replacing sericite (fine grained muscovite) grains. Except for those minerals, some pyrophyllite occurs in the sericite-pyrite-quartz alteration zone, and the rutile is widespread from the biotite alteration to alunite alteration zones. Biotite, sericite, and chlorite are typical porphyry stage alteration minerals [24]. It is typical that these porphyry alteration stage minerals are overprinted by epithermal alteration minerals in the Tiegelongnan deposit, and these minerals formed in different occurrences, such as breccia, vein-filling, or as replacement, which corresponds with the multiple dating results on the altered minerals. Biotite and sericite display a ^{40}Ar - ^{39}Ar age at ~121 Ma, whereas alunite indicates the age ranging from 117 to 100 Ma [21]. Alunite-kaolinite-dickite breccia is late epithermal stage products, breaking earlier phyllitic altered rocks (Figure 3a). Kaolinite-dickite veins cut the early phyllitic and biotite alteration stages' quartz-sulfide veins. However, they are most commonly shown as kaolinite filling in biotite veins (Figure 3b), and kaolinite fills the barren quartz-pyrite veins in phyllitic alteration zone (Figure 3c). Kaolinite also replaces fine muscovite grains in the phyllitic alteration zone (Figure 3d). In some cases, a mineral sequence is shown as a single vein, firstly with quartz crystallizing, followed by alunite alteration, and ending up with kaolinite crystalized in the center of the vein. This alunite, kaolinite, and dickite assemblage was documented as acidic minerals and epithermal products in condition of low temperature and low pH value [25].

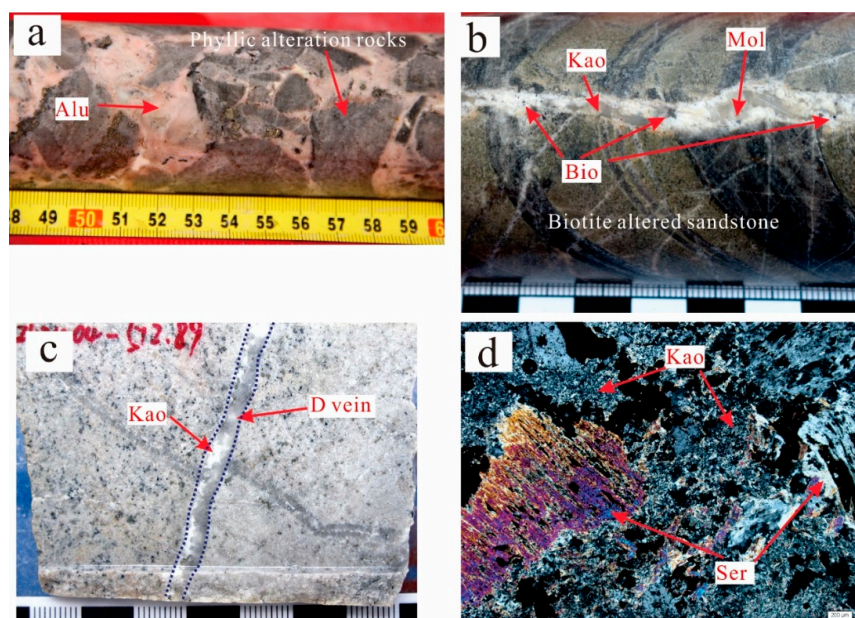


Figure 3. The epithermal alteration overprinted on the porphyry alteration. (a) Alunite breccia break through phyllitic altered and mineralized host rocks, (b) kaolinite vein crosscutting biotite altered host rocks and filling in biotite-molybdenite vein, (c) kaolinite filling in cavity of quartz-pyrite vein, (d) sericite replaced by kaolinite grains. Alu: alunite, Bio: biotite, Ser: sercite, Kao: kaolinite, Mol: molybdenite.

3.2. Mineralization

Chalcopyrite, bornite, and pyrite are sulfide assemblage precipitating in biotite and phyllitic alteration zone with minor molybdenite, whereas the Cu (Fe)-As-S minerals enargite, tennantite, and Cu-S covellite, digenite are the dominant sulfides in advanced argillic alteration zone [26,27]. Chalcopyrite and bornite in the biotite and phyllitic alteration zone are the main Cu mineralization of the porphyry stage, including quartz-chalcopyrite ± bornite veins and disseminated chalcopyrite and bornite. This is the main porphyry Cu orebody, hosted as quartz-sulfides veins, and disseminated sulfides in wall rocks. The enargite-tennantite-covellite-digenite assemblage mostly occurs in the alunite and kaolinite alteration zone, which are the products of the high-sulfidation epithermal Cu orebody [8]. Epithermal stage Cu sulfides are mainly presented as alunite-kaolinite-sulfides veins.

These two stages of sulfide mineral assemblages display a complicated overprinting and cross-cutting relationship. Kaolinite-sulfide veins crosscut quartz veins (Figure 4a), those sulfides are mostly Cu (Fe)-(As)-S minerals, also some chalcopyrite and bornite were reported as result of solid solution from those minerals [25]. Under the microscope, we find some enargite filling in the fractures of quartz veins along with kaolinite. The pyrite occurs as early phyllitic alteration product, because it is the most easily being replaced by the enargite. Replacement textures of chalcopyrite, bornite, and pyrite affected by Cu (Fe)-As-S and Cu-S minerals are common in the Tiegelongnan deposit. The pyrite is replaced from the edge firstly by bornite, and then the bornite is replaced by digenite and covellite (Figure 4b). Enargite and tennantite replace chalcopyrite (Figure 4c). There are some arguments that replacement relationship between sulfides is supergene replacement textures, because covellite and digenite are typical supergene sulfides also. However, $\delta^{65}\text{Cu}$ of covellite and digenite in the Tiegelongnan are averaging at 0.25‰ [28], which is similar to the hypogene copper sulfides $\delta^{65}\text{Cu}$ value [29]. In some cases, the Cu (Fe)-As-S and Cu-S minerals are filled in the fractures instead of replacing Fe-bearing minerals (Figure 4d), which might indicate a brittle force condition before the epithermal mineralization. This corresponds with the alunite and kaolinite breccia in Figure 3a. The Cu (Fe)-As-S and Cu-S sulfides even cut through post-mineral porphyry and breccia rocks. Generally, overprinting of the Cu (Fe)-As-S and Cu-S on chalcopyrite-bornite-pyrite assemblage is common in the Tiegelongnan deposit, and it was demonstrated in different occurrences, including the former replacing the latter minerals, the former filling in fractures of the latter sulfides, and the former cutting the chalcopyrite-bornite mineralized rocks or veins.

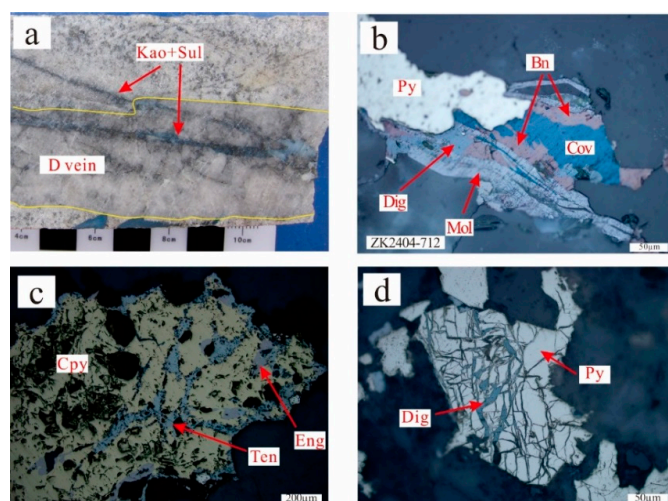


Figure 4. Textures of epithermal sulfides overprinting porphyry sulfides. (a) Kaolinite-sulfide veinlets cross-cut quartz-pyrite veins, (b) later covellite and digenite replacing boronite and pyrite, (c) tennantite and engargite replacing chalcopyrite, (d) pyrite fractures filled with digenite. Bn: bornite; Cpy: chalcopyrite, Cov: covellite, Dig: digenite, Eng: enargite, Mol: molybdenite; Kao: kaolinite, Py: pyrite, Sul: sulfides, Ten: tennantite.

4. Structures

The Tiegelongnan deposit and most of other deposits in the Duolong district are along the NE–SW faults. It is widely accepted that these faults mainly controlled the emplacement of magma and hydrothermal fluids in the Duolong district [30]. However, there were few convincing studies clarifying the overlying volcanic rocks which conceal the whole porphyry and epithermal ore bodies. The NW–SE faults, named as Rongna Fault, are characterized by geomorphologically linear sunken terrain, valleys, with fault springs seen at the ground level. In the deposits area, the fault occurred as a river valley, which is called the Rongna Valley (Figure 5). The fault divides the Meiriqiecuo Formation andesite into two parts, suggesting the structural movement took place after andesite eruption, which is dated at ~110 Ma [8].

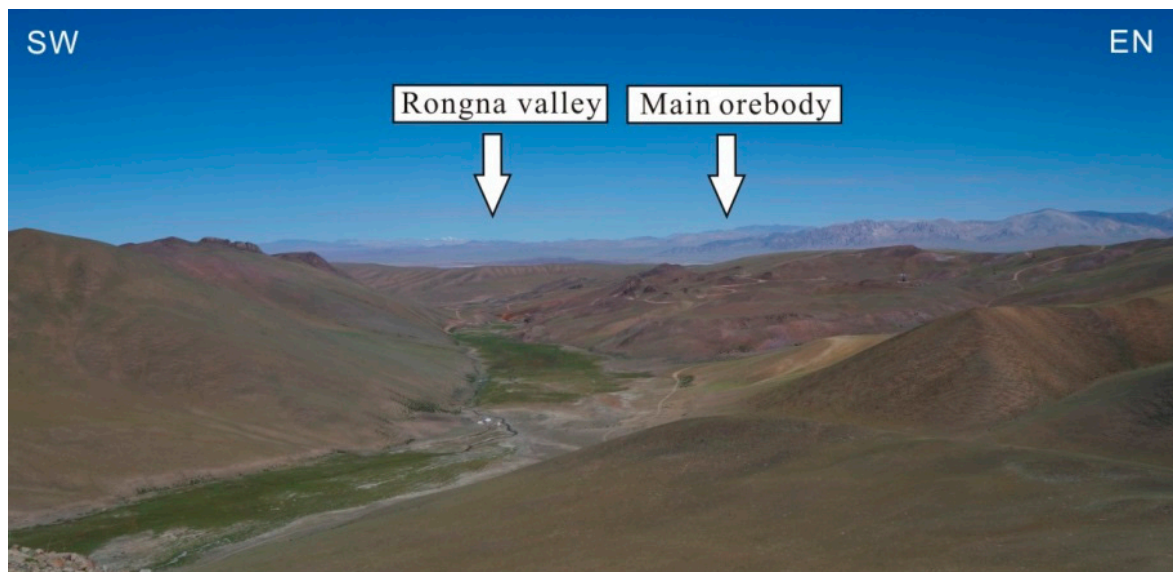


Figure 5. Rongna Valley, topography of the Rongna fault in the Tiegelongnan deposit.

The audio-frequency magneto-telluric method (AMT) was applied to understand the fault features, and further to predict the occurrences of the orebody in a deep level on the south side. From the AMT tests, electrical properties of different rocks obviously vary from each other in the Tiegelongnan deposit. The Cretaceous volcanic cap-rocks have low polarizability, whereas extremely high resistivity is shown in the paleo-weathering crust. The Jurassic sandstone showed low resistivity and high polarization, while the advanced argillic altered sandstone has high resistivity. We found the >0.5% grade Cu whole porphyry and epithermal orebodies correspondent with the low resistivity zone (Figure 6). There are two low-resistivity anomalies (C1 and C2) in the E103 AMT cross-section and the C1 anomaly coincides with the explored orebody. Therefore, the C2 low-resistivity anomaly could be another part of the whole orebody. The fault plane shown in the AMT cross-section is dipping to the south with an angle of 70° to 80° (Figure 6).

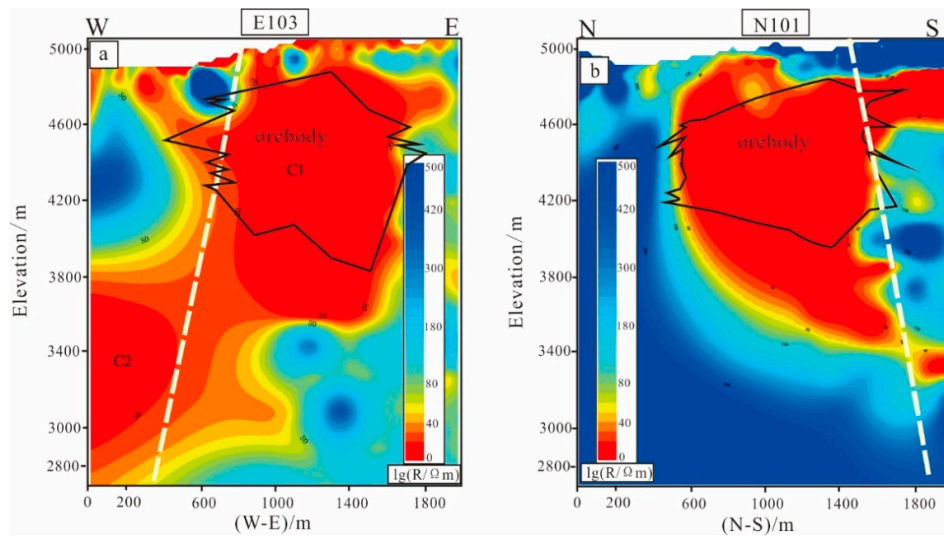


Figure 6. 2D inversion resistivity section of the audio-frequency magneto-telluric method (AMT) test (a) north–south cross-section; (b) east–west cross-section.

5. Post-Mineral Weathering and Erosion

The epithermal Cu (Au) mineralization orebody found by diamond drilling is covered by the Meiriqiecuo Formation volcanic rocks (Figure 7a). The dome-shaped and gently dipping andesite layer was discovered by drilling at an elevation of 5110–4930 m above sea level at the ground surface and 5080–4620 m at the bottom. The average thickness of the andesite is 90 m, thinning from southwest to northeast (Figure 7b).

A layer of weathered paleosoil is observed between the andesite and the underlying porphyry and epithermal Cu (Au) orebodies, which suggests that prominent weathering occurred after mineralization before the overlying andesite. Three types of erosional surfaces are recognized (Figure 8). The first type is a weakly weathered eluvium without movement, containing detrital sandstone, with some malachite and azurite. The second type of erosional surface is residual ancient soil, defined as a complex of clay soil and illuvial soil with a small amount of debris, which is generally formed in the watershed or on slope landforms. The third type is slope washes, which is weakly weathered eluvial material transported by water, accumulated on a slope, and incorporated rounded fragments of the basement. Slope washes form in the transitional area between erosional and depositional zones in this area.

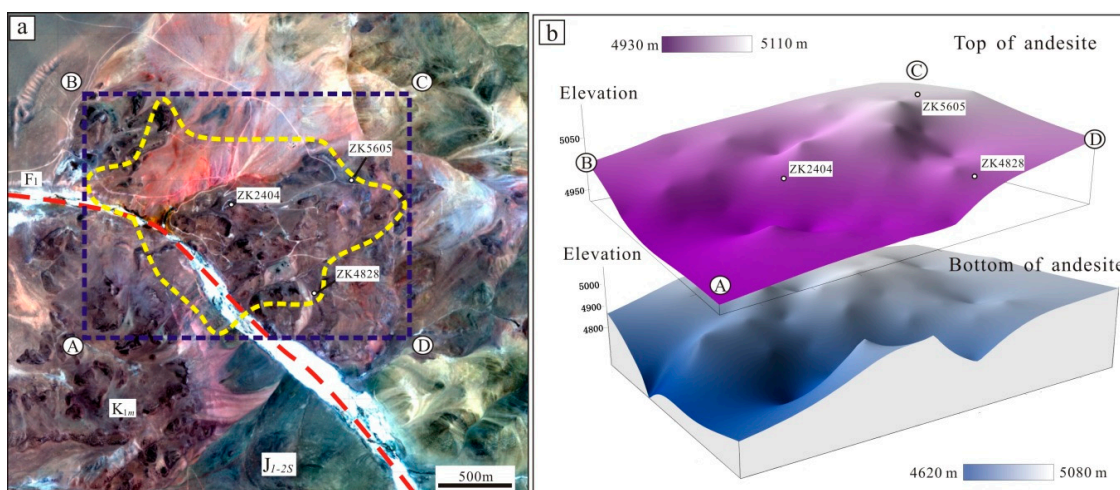


Figure 7. (a) High-resolution remote sensing image, and (b) a 3-D map of the Meiriqiecuo Formation andesite [31]. Red dotted lines: faults; the yellow dotted line: the boundary of the mineralized body.

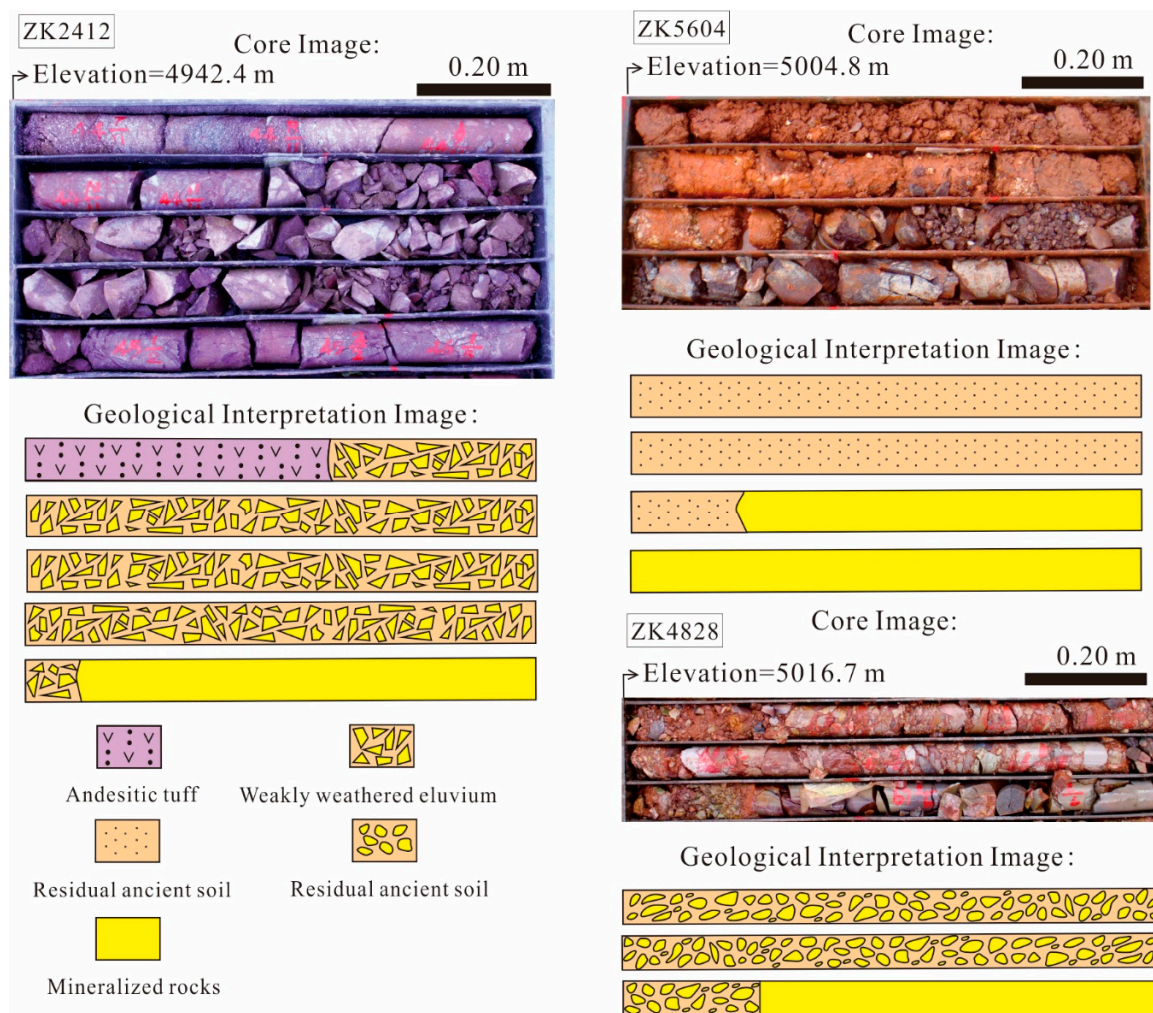


Figure 8. Photographs of typical weathering paleo-crusts in the Tiegelongnan deposit. ZK2412—The first type weathering weakly weathered eluvium. ZK5604—The second type weathering residual ancient soil. ZK4828—The third type weathering slope washes.

6. Discussion

6.1. Magmatism Indication of Tectonic Setting in the Duolong District

The Bangong–Nujiang ocean crust has started subducting northwards beneath the southern Qiangtang terrane since the Middle Jurassic. This leads to the formation of the large intermediate to felsic magmatic arc that emplaced inboard of the southern continental margin of the south Qiangtang terrane in the Middle to Late Jurassic (170–145 Ma) [32–36]. Some authors argued that the Bangong–Nujiang oceanic crust may subduct in two directions, both northward beneath southern Qiangtang Terrane and southward beneath northern Lhasa Terrane, respectively [36,37]. From 145 to 130 Ma, however, there is a noticeable magmatic gap in the southern Qiangtang terrane. Similar magmatic gaps occur in the Andes [38] and southern Gangdese areas [39] in response to the low-angle or flat-slab subduction of the oceanic crust. After that, the Bangong–Nujiang oceanic basin was closed. Although the closure time is controversial, it is generally accepted as the period from Middle Jurassic to Late Cretaceous [12,40–43]. Recent research narrowed the closure time within 10 Ma from 140 Ma to 130 Ma [37]. Based on the time constraints, it suggests that the collision between the Qiangtang and Lhasa terranes occurred through an arc–arc ‘soft’ collision from the east to the west after the BNO closure [32,40,41]. The Jurassic to Lower Cretaceous (<125 Ma) marine sedimentary rocks were

transposed, intruded by granitoids, and were uplifted above sea level before around 118 Ma [40]. The extensive magmatism in the Duolong district is associated with the Qiangtang–Lhasa collision event [9,37].

Numerous igneous rocks such as gabbro, basalt, basaltic andesite, andesites, rhyolite, and intermediate to felsic porphyries are widely distributed in vicinity of the Tiegelongnan deposit. Zircon U-Pb ages of the porphyry intrusions in the Tiegelongnan deposit range from 115.9 Ma to 123.1 Ma, which is consistent with the mineralization (molybdenite Re-Os) ages (119.0 ± 1.4 Ma [20]; 121.2 ± 1.2 Ma [8]). This is also consistent with porphyry intrusions and mineralization ages of other deposits in the Duolong district, such as Bolong and Duobuza deposits [17]. They are temporally associated with this younger generation of magmatic emplacement which is related with the Qiangtang–Lhasa collision. Intrusion rocks geochemistry and isotope studies have been conducted to understand the genetic association between those porphyry deposits and tectonic settings. Geochemistry data mostly obtained from the ore-bearing porphyritic intrusions in the Duolong district indicate they are magmatic rocks and adakite-like rocks [11,14,44,45]. They have relatively high oxygen fugacity (f_{O_2}) and high H₂O contents that are critical to the formation of porphyry and epithermal deposits [46]. During the process of magma upwelling, adakite-like melts might get mixed with large amount of copper and other metals and sulfur from either interaction with hot peridotite in the mantle wedge region [47] or mixing with mantle-derived melts [48]. It eventually resulted in mantle-derived juvenile materials, which are thought to bring heat and materials to generate juvenile mafic lower crust. The magmas experience various degrees of fractional crystallization and crustal contamination during its emplacement, when it is derived from the remelting of the juvenile mafic lower crust as a result of previous arc magmatism. Some of these hybrid magmas formed calc-alkaline ore bearing porphyries via the shallow magma emplacement, leading to the formation of giant porphyry and epithermal Cu (Au) deposits [49–52].

The Jurassic (170–145 Ma) intermediate–felsic intrusive rocks of the southern Qiangtang terrane primarily exhibit negative whole-rock $\varepsilon_{Nd}(t)$ and zircon $\varepsilon_{Hf}(t)$ and old Hf isotope crustal model ages, indicating that those Jurassic rocks were largely derived from mature or recycled continental crust materials [35,36,53]. This is compatible with what been observed in the Early Cretaceous Fuye pluton, Caima pluton and Qingcaoshan pluton in the Qiangtang Terrane [53]. In contrast, $\varepsilon_{Nd}(t)$ and $\varepsilon_{Hf}(t)$ value and Hf isotope model ages of the Early Cretaceous (~126–116 Ma) magmatic rocks from the Duolong district indicate they were probably derived from magma as a mixture of the juvenile lower crust and mature crustal materials [9]. In addition, previous studies on Pb isotopic compositions of the porphyry intrusions, sulfides, and sulfate in the Tiegelongnan deposit suggest that the Pb of this deposit is mainly derived from a crust–mantle mixed subduction zone [26,54,55].

Although there is no specific research on the geochemistry of the porphyry intrusions in the Tiegelongnan deposit, owing to their strong alteration and leaching erasing its geochemical signature, the features of the intrusions in the Duolong district could represent that in the Tiegelongnan deposit. Thus, it suggests that plenty of juvenile crust materials are involved in the intrusions in the Tiegelongnan porphyry Cu (Au) deposit. The juvenile crust materials have been becoming gradually dominated during the Late Mesozoic since the vertical growth and thickening of the continental crust of the southern Qiangtang terrane during the Early Cretaceous [9,56]. It is commonly accepted that variable sources conjunctly contributed to the formation of magma in this district [53]. The dominant crust signature from radiogenic isotopes is reported as features of the post-subduction products, which is well explained by Richards (2009) [57]. All of these suggest that magmatism and mineralization of the Tiegelongnan porphyry Cu (Au) deposit probably occurred in an active continental margin environment after the subduction of BNO plate, as result of continental crust thickening and terranes collision (Figure 9).

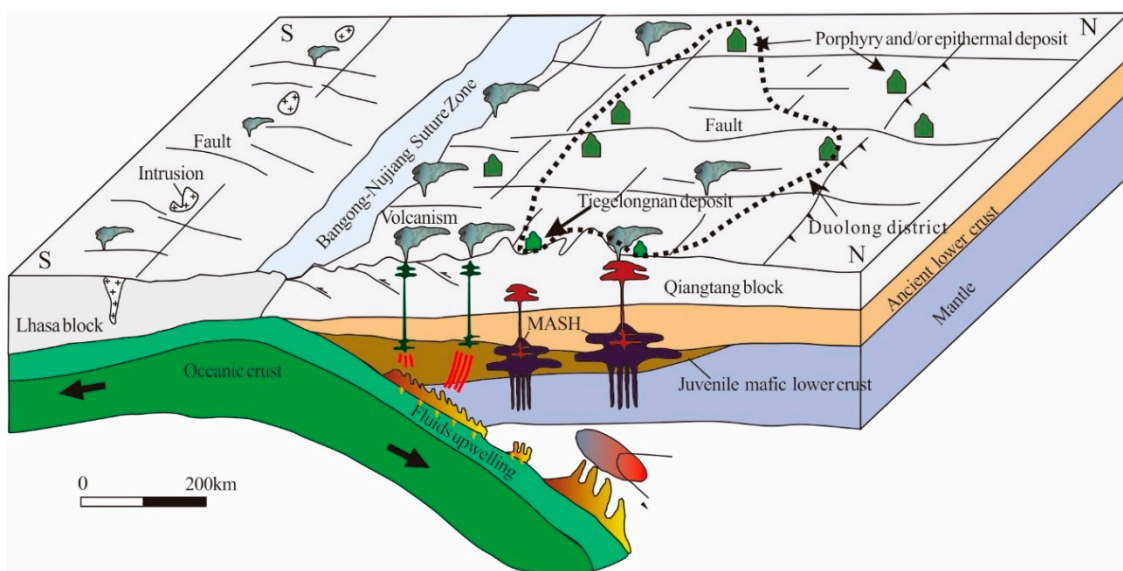


Figure 9. Tectonic setting model for the formation of the Duolong deposit, Tibet.

6.2. Tectonic Reconstruction of Epithermal Overprinting Porphyry

The continental crust thickening resulted from the Qiangtang–Lhasa collision might be the reason for the emplacement of magma and formation of porphyry deposits in the Duolong district. An extensional condition is common during the post-subduction stage of two plates or terranes [57], thus Sillitoe and Hedenquist (2003) explained that some arcs are subjected to neutral stress condition or mild extension where high-sulfidation epithermal deposits formed [23]. This might be one of the reasons that porphyry mineralization is overprinted by epithermal mineralization in the Tiegelongan deposit. Besides, water table decline is another possible reason for epithermal mineralization formed at deep level where porphyry mineralization formed earlier at depth [58]. The paleosoil occurred between the whole mineralization Cu orebody and the overlying andesite in the Tiegelongan deposit indicates weathering and erosion took place before andesite covering at 110 Ma, which is possible to decrease the water table. Furthermore, fluid inclusion pressure evidence suggests that rapid mountains lifting and erosion took place between two stages of porphyry intrusions at 121 and at 116 Ma respectively in the Tiegelongan deposit [22]. The occurrences of overprinting of epithermal on porphyry alteration and mineralization in the Tiegelongan deposit are mainly characterized by veins and fracture filling, and the replacement between the typical minerals of two episodes. From the absolute geochronology data, alunite was formed between 117 and 100 Ma, which postdates the ages of biotite and sercrite at 121 Ma [21]. Early formed veins were reopened under an extensional situation, giving channels for later epithermal fluids. Reopening of early formed textures can improve rock permeability. It enables magmatic-hydrothermal fluid to cool with low temperature isotherm dropping. When the isotherm line decline to deep level of earlier formed porphyry deposit, epithermal minerals formed and replaced porphyry minerals. Specifically, the low temperature minerals alunite and kaolinite and high sulfidation state sulfides (tenantite, enargite, digenite, covellite, etc.) precipitated and replaced porphyries stage alteration and sulfide minerals at a higher temperature and in a deeper level. Although most porphyry deposits are formed in convergent and compressive settings [49], high sulfidation epithermal can be generated in calc-alkaline andesitic-dacitic arcs under neutral stress or mild extension conditions [23]. During the formation of this porphyry and epithermal deposit, the extensional strain in the Duolong district might be related with the Bangong–Nujiang subduction zone retreating after the BNO closure [9,10,44].

During the epithermal stage, some breccia formed, and straight veins break phyllitic altered rocks, indicate that epithermal events overprinting on the porphyry events. Plenty of breccia implies that rocks are brittle in the epithermal stage. Hydrothermal processes in ductile and brittle rocks in a

magmatic–epithermal environment study suggest that the ductile-brittle transition commonly occurs about 370–400 °C [59]. This is higher than epithermal hydrothermal fluid temperature 160–270 °C [6]. Therefore, before epithermal events taking place, the wall rocks of the Tiegelongnan deposit is brittle and could be easily broken by the accumulation of hydrothermal fluid or by fault events in the Duolong district. This gives access to epithermal fluid arriving at shallow sites, and overprints porphyry system along those faults, fractures, and other opened space.

6.3. Post-Mineral Erosion and Preservation

The crust thickening and terranes collision in the Bangong–Nujiang suture zone, combining with later coming India–Asia plate collisions, resulted in rapid uplifting and erosion of the deposits in the Duolong district. It also affects the uplifting and erosion of most parts of the Tibetan Plateau [33,41]. The large-scale uplift was activated by the Lhasa–Qiangtang collision [60,61], that resulted in the angular unconformity contact between the continental Abushan Formation and the underlying marine sediments [33]. The erosion of the Tiegelongnan deposit happened right after its formation, which is observed from the weathered rocks under the andesite. The fluid inclusion study suggested the eroded layers may reach a thickness of 600–1200 m before cover of the andesite at 110 Ma [27]. In the following exhumation rate calculations, the youngest formation age of the Tiegelongnan deposit was used at ~118 Ma dated from the molybdenite. The exhumation rate of ground surface increased with the elevation [62] and it has functional relationship with elevation. The smallest exhumation thickness and interval of the protection can be used to calculate the smallest exhumation rate. Thus the Tiegelongnan deposit has experienced exhumation for 6 to 7 m.y. and the exhumation rate is 0.1–0.2 mm/y.a, averagely at 0.15 mm/y.a. This is consistent with the common exhumation rate of the epithermal deposit at ~0.167 mm/y.a, and the porphyry deposit at 0.158 mm/y.a [63].

Northern Tibet has been elevated more than 5000 m, and it is continuously affected by the India–Asia collision system, thus leading to a more intensive exhumation than other parts of Tibet, while the southern Tibetan Plateau attained a 3–4 km elevation at ~99 Ma [64]. The Tiegelognnan deposit was overlain by the andesite after small interval of exhumation which protected the Tiegelongnan deposit from totally erosion. The erosion after andesite settle is still non-negligible. The apatite HeFTy program [65] was used to model the prolonged thermal history of the Tiegelongnan deposit [66]. It suggested that the Tiegelongnan deposit has experienced four cooling stages: (i) relatively slow cooling from Early Cretaceous to Late Cretaceous (120–75 Ma); (ii) fast cooling in Late Cretaceous (75–60 Ma); (iii) moderately fast cooling from Eocene to Oligocene (45–30 Ma); (iv) very fast cooling since Late Miocene (<7.8 Ma). The exhumation thickness is at least 3600 m since Late Cretaceous in the Duolong district. Yin et al., (2000) and Kapp et al., (2007) reported the subsequent India–Asia collision led to 1400 km of shortening within recent 70 m.y. [40,41]. The andesite has a thickness of ~500 m [67], which is not thick enough to withstand that intensive exhumation. Therefore, the andesite is not the solely protective cover for the Tiegelongnan deposits. Post-mineral sediments, such as the Upper Cretaceous Abushan Formation (K_2a) and the Upper Oligocene Kangtuo Formation (E_3k), might also act as significant caps for protecting orebodies.

Along with the thickening of the continental arc, collapse of the crust may destruct the whole porphyry and epithermal Cu (Au) orebodies. The Rongna Fault might be the result of the collapse of the accumulated crust rocks. The inversion resistivity cross-section in Figure 6a showed that a normal high angle fault breaks the high resistivity zone into two separated C1 and C2 zones. It also cuts through the andesite from the Rongna Valley, and may dislocate and conceal the western part of the Cu (Au) orebody to deeper places.

A simplified model (Figure 10) was applied to describe the porphyry Cu system in the Tiegelongnan deposit. Epithermal Cu (Au) mineralization veins are mostly retained in the advanced argillic alteration zone, which overprints phyllitic alteration zone on top of porphyry Cu orebody (Figure 10a). This is a transitional zone between the disseminated high-sulfidation epithermal precious metal deposit and the porphyry Cu (Au) orebody (Figure 10b). There might have been disseminated

epithermal precious metal deposit existing in theory. The reason of not being detected on the deposit is that it either was not well preserved because of severe erosion or has not been found yet. Deep in the porphyry Cu (Au) system, the bottom of the porphyry Cu orebody has not been detected yet. We suggest there could be economic potential at depth, because biotite alteration is shown at depth, if it could represent the typical potassic alteration, which usually is the core of mineralization orebody in the porphyry Cu system [68]. Obviously, we did not reveal the whole biotite alteration, which might be concealed at a deeper level.

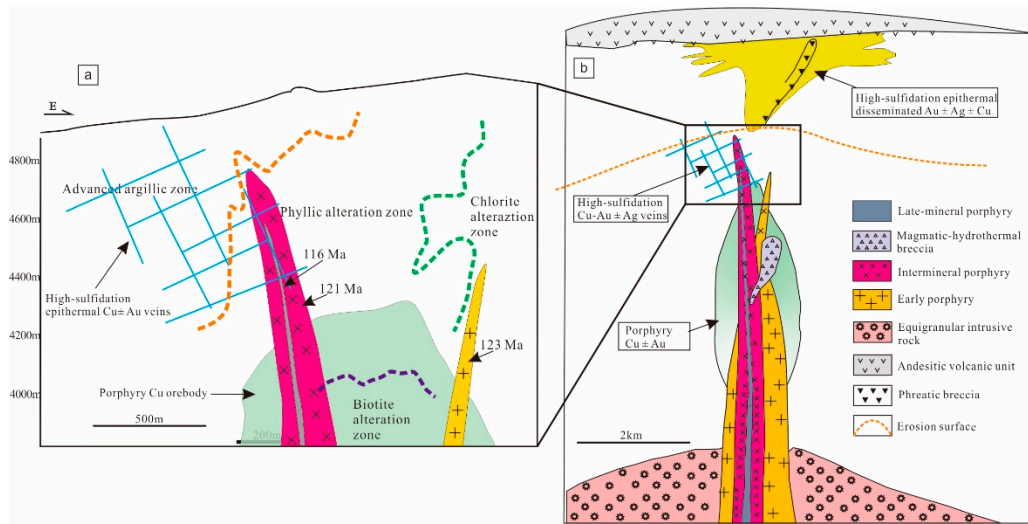


Figure 10. (a) Simplified geology map of the A-B sections in Tiegelongnan [31]. (b) Anatomy of a condensed porphyry Cu system showing the spatial interrelationships of porphyry Cu orebody, high-sulfidation epithermal Cu ± Au orebody, and late-mineralization andesitic volcanic rocks [31].

7. Implications and Conclusions

The geological history of the Tiegelongnan deposit is as follows: (i) Early Jurassic active continental margin sandstone (pre-mineral stage); (ii) emplacement of multiple porphyry intrusions and formation of the porphyry ore system (first mineral stage); (iii) overprinting of epithermal alteration and mineralization (second mineral stage); (iv) weathering and erosion (≥ 600 m) and volcanic extrusion (preservation); (v) continuous lifting and erosion/movement of the Rongna fault (dislocation). This process is associated with the movement of the Bangong–Nujiang oceanic plate, following Qiangtang–Lhasa terranes collision and the effect of the India–Lhasa terranes subduction and collision. Marine sandstone was deposited before or during subduction of the oceanic plate in Jurassic. Igneous rocks emplacement and eruption are the results of the subduction of oceanic plate during 170–145 Ma, and the Qiangtang–Lhasa terrane collision between 126 and 116 Ma. Hydrothermal fluid is induced by those porphyry intrusions, and it contributes to porphyry mineralization. Shortly after that, younger stage of epithermal fluid overprinted the porphyry mineralization because of erosion of the system due to the extensional structures at around 116 Ma. With continuous collision of Qiangtang and Lhasa terranes, rapid lifting and strong exhumation partly eroded the ore deposit. Volcanic andesite (~110 Ma) covered on the top of the orebody protects it from entire erosion. Subsequent India and Lhasa plates subduction and collision uplifted the plateau and caused the erosion of those deposits in the Duolong district again. Post-mineral structure such as the Rongna Fault possibly dislocated the main orebody of the Tiegelongnan deposit (Figure 6a).

This review of the Tiegelongnan deposit is significant for the future exploration programs, even for exploration of porphyry and epithermal deposits in the Duolong district or even the Bangong–Nujiang suture zone. The Rongna Fault dislocated the Tiegelongnan deposit in its western part. Another part of the orebody on the hanging wall of the fault might slip southwestward and be concealed

to a deeper domain. The nearly 11 Mt of Cu resource currently being explored might be part of the entire Tiegelongnan porphyry and epithermal Cu (Au) orebody, which is similar to the San Manuel-Kalamazoo porphyry copper deposit in South America [69]. Comparably, we are confident on the great potential of the Tiegelongnan deposit. Further understanding of the dislocation of the Rongna Fault should be conducted later, which would contribute to increasing the ore reserves of the deposit at depth.

The volcanic rocks unconformably overlie on the whole porphyry and epithermal Cu (Au) orebody, which prevents the orebody from being subject to further erosion. This might be the reason for only epithermal copper orebody being found at the top the Tiegelongnan deposit so far, but not anywhere else. There might be epithermal mineralization on the Duobuza and Bolong deposits, but they might be fully eroded away due to the lack of overlying protection. Furthermore, due to the large range of volcanic rocks in the Duolong district, more porphyry and epithermal copper and gold deposits are of great potential to be preserved, and that could be the future exploration direction in the Duolong district.

Author Contributions: Y.S. carried out the project and coordinated this study. All authors took part in the field work, analyzed the results and wrote the manuscript; Y.S. and C.Y mainly revised and edited the paper.

Funding: This research was partly funded by the National Key R & D Program of China (No. 2018YFC0604106), the National Natural Science Foundation of China (No. 41402178), and the Chinese Geological Survey Program (DD20160026).

Acknowledgments: We thank three anonymous reviewers, the Editor Shi, and the academic editor of *Minerals* Alain Chauvet for their positive and constructive comments that are helpful to improve the manuscript significantly. Qing Zhang from the University of Wollongong provided major contributions to the English editing of the paper.

Conflicts of Interest: The authors declare no conflict of interest.

References and Notes

1. Hou, Z.; Xie, Y.; Xu, W.; Li, Y.; Zhu, X.; Khin, Z.; Beaudoin, G.; Rui, Z.; Huang, W.; Luo, C. Yulong deposit, eastern Tibet: A high-sulfidation Cu-Au porphyry copper deposit in the eastern Indo-Asian collision zone. *Int. Geol. Rev.* **2007**, *49*, 235–258.
2. Yang, A.; Hou, Z.; White, C.N.; Chang, Z.; Li, Z.; Song, Y. Geology of the post-collisional porphyry copper–molybdenum deposit at Qulong, Tibet. *Ore Geol. Rev.* **2009**, *36*, 133–159. [[CrossRef](#)]
3. Zheng, W.; Tang, J.; Zhong, K.; Ying, L.; Leng, Q.; Ding, S.; Lin, B. Geology of the Jiama porphyry copper–polymetallic system, Lhasa Region, China. *Ore Geol. Rev.* **2016**, *74*, 151–169. [[CrossRef](#)]
4. Zhu, X.; Li, G.; Chen, H.; Ma, D.; Zhang, H.; Zhang, H.; Liu, C.; Wei, L. Petrogenesis and metallogenetic setting of porphyries of the Duobuza porphyry Cu–Au deposit, central Tibet, China. *Ore Geol. Rev.* **2017**, *89*, 858–875. [[CrossRef](#)]
5. Zhu, X.; Li, G.; Chen, H.; Ma, D.; Huang, H. Zircon U–Pb, Molybdenite Re–Os and K-feldspar $^{40}\text{Ar}/^{39}\text{Ar}$ Dating of the Bolong Porphyry Cu–Au Deposit, Tibet, China. *Resour. Geol.* **2015**, *65*, 122–135. [[CrossRef](#)]
6. Hedenquist, J.W.; Arribas, A.; Gonzalez-Urrien, E. Exploration for epithermal gold deposits. *Rev. Econ. Geol.* **2000**, *13*, 245–277.
7. Tang, J.; Sun, X.; Ding, S.; Wang, Q.; Wang, Y.; Yang, C.; Chen, H.; Li, Y.; Li, Y.; Wei, L.; et al. Discovery of the epithermal deposit of Cu (Au–Ag) in the Duolong ore concentrating area, Tibet. *Acta Geosci. Sin.* **2014**, *35*, 6–10. (In Chinese) [[CrossRef](#)]
8. Lin, B.; Tang, J.-X.; Chen, Y.-C.; Song, Y.; Hall, G.; Wang, Q.; Yang, C.; Fang, X.; Duan, J.-L.; Yang, H.-H. Geochronology and Genesis of the Tiegelongnan Porphyry Cu (Au) Deposit in Tibet: Evidence from U–Pb, Re–Os Dating and Hf, S, and H–O Isotopes. *Resour. Geol.* **2017**, *67*, 1–21. [[CrossRef](#)]
9. Wei, S.-G.; Tang, J.-X.; Song, Y.; Liu, Z.-B.; Feng, J.; Li, Y.-B. Early Cretaceous bimodal volcanism in the Duolong Cu mining district, western Tibet: Record of slab breakoff that triggered ca. 108–113 Ma magmatism in the western Qiangtang terrane. *J. Asian Earth Sci.* **2017**, *138*, 588–607. [[CrossRef](#)]
10. Geng, Q.; Zhang, Z.; Peng, Z.; Guan, J.; Zhu, X.; Mao, X. Jurassic–Cretaceous granitoids and related tectono-metallogenesis in the Zapug–Duobuza arc, western Tibet. *Ore Geol. Rev.* **2016**, *77*, 163–175. [[CrossRef](#)]

11. Li, J.X.; Qin, K.; Li, G.; Xiao, B.; Zhao, J.; Chen, L. Petrogenesis of Cretaceous igneous rocks from the Duolong porphyry Cu–Au deposit, central Tibet: Evidence from zircon U–Pb geochronology, petrochemistry and Sr–Nd–Pb–Hf isotope characteristics. *Geol. J.* **2016**, *51*, 285–307. [[CrossRef](#)]
12. Pan, G.; Wang, L.; Li, R.; Yuan, S.; Ji, W.; Yin, F.; Zhang, W.; Wang, B. Tectonic evolution of the Qinghai-Tibet plateau. *J. Asian Earth Sci.* **2012**, *53*, 3–14. [[CrossRef](#)]
13. Zhu, D.; Zhao, Z.; Niu, Y.; Dilek, Y.; Hou, Z.; Mo, X. The origin and pre-Cenozoic evolution of the Tibetan Plateau. *Gondwana Res.* **2013**, *23*, 1429–1454. [[CrossRef](#)]
14. Ding, S.; Chen, Y.; Tang, J.; Zheng, W.; Lin, B.; Yang, C. Petrogenesis and Tectonics of the Naruo Porphyry Cu (Au) Deposit Related Intrusion in the Duolong Area, Central Tibet. *Acta Geol. Sin.* **2017**, *91*, 581–601. [[CrossRef](#)]
15. Li, J.; Qin, K.; Li, G.; Noreen, J.; Zhao, J.; Cao, M.; Huang, F. The Nadun Cu–Au mineralization, central Tibet: Root of a high sulfidation epithermal deposit. *Ore Geol. Rev.* **2016**, *78*, 371–387. [[CrossRef](#)]
16. Li, G.; Li, J.; Qin, K.; Duo, J.; Zhang, T.; Xiao, B.; Zhao, J. Geology and Hydrothermal Alteration of the Duobuza Gold-Rich Porphyry Copper District in the Bangongco Metallogenic Belt, Northwestern Tibet. *Resour. Geol.* **2012**, *62*, 99–118. [[CrossRef](#)]
17. Lin, B.; Chen, Y.; Tang, J.; Wang, Q.; Song, Y.; Yang, C.; Wang, L.; He, W.; Zhang, L. $^{40}\text{Ar}/^{39}\text{Ar}$ and Rb-Sr Ages of the Tiegelongnan Porphyry Cu-(Au) Deposit in the Bangong Co-Nujiang Metallogenic Belt of Tibet, China: Implication for Generation of Super-Large Deposit. *Acta Geol. Sin.* **2017**, *91*, 602–616. [[CrossRef](#)]
18. Li, G.; Duan, Z.; Liu, B.; Zhang, H.; Dong, S.; Zhang, L. The discovery of Jurassic accretionary complexes in Duolong area, northern Bangong Co-Nujiang suture zone, Tibet, and its geologic significance. *Geol. Bull. China* **2011**, *30*, 1256–1260. (In Chinese)
19. Liu, Y.; Wang, M.; Li, C.; Xie, C.; Chen, H.; Li, Y.; Fan, J.; Li, X.; Xu, W.; Sun, Z. Cretaceous structures in the Duolong region of central Tibet: Evidence for an accretionary wedge and closure of the Bangong–Nujiang Neo-Tethys Ocean. *Gondwana Res.* **2017**, *48*, 110–123. [[CrossRef](#)]
20. Fang, X.; Tang, J.; Song, Y.; Yang, C.; Ding, S.; Wang, Y.; Wang, Q.; Sun, X.; Li, Y.; Wei, L.; et al. Formation epoch of the South Tiegelong superlarge epithermal Cu (Au-Ag) deposit in Tibet and its geological implications. *Acta Geosci. Sin.* **2015**, *36*, 168–176. (In Chinese)
21. Yang, C.; Beaudoin, G.; Tang, J.; Song, Y. An extreme long life span of porphyry and epithermal Cu deposit: The Tiegelongnan deposit, Tibet, China. 2018; in preparation.
22. Yang, C.; Beaudoin, G.; Tang, J.; Song, Y. Geology and genesis of Tiegelongnan porphyry and epithermal base metal deposit in Duolong district, Tibet, China: From stable isotope and fluid inclusions constrains. 2018; in preparation.
23. Sillitoe, R.H.; Hedenquist, J.W. Linkages between volcanotectonic settings, ore-fluid compositions, and epithermal precious metal deposits. *Spec. Publ. Soc. Econ. Geol.* **2003**, *10*, 315–343.
24. Seedorff, E. Porphyry deposits: Characteristics and origin of hypogene features. *Econ. Geol.* **2005**, *29*, 251–298.
25. Stoffregen, R. Genesis of Acid-Sulfate Alteration and Au-Cu-Ag Mineralization at Summitville, Colorado. *Econ. Geol.* **1987**, *82*, 1575–1591. [[CrossRef](#)]
26. Wang, Y.; Tang, J. The First Discovery of Colusite in the Tiegelongnan Supper-large Cu (Au, Ag) Deposit and Significance for the Genesis of the Deposit. *Acta Geol. Sin.* **2018**, *92*, 400–401. [[CrossRef](#)]
27. Yang, C.; Tang, J.; Wang, Y.; Yang, H.; Wang, Q.; Sun, X.; Feng, J.; Yin, X.; Ding, S.; Fang, X.; et al. Fluid and geological characteristics researches of Southern Tiegelong epithermal porphyry Cu-Au deposit in Tibet. *Miner. Depos.* **2014**, *33*, 1287–1305. (In Chinese)
28. Duan, J.; Tang, J.; Li, Y.; Liu, S.; Wang, Q.; Yang, C.; Wang, Y. Copper isotopic signature of the Tiegelongnan high-sulfidation copper deposit, Tibet: Implications for its origin and mineral exploration. *Miner. Depos.* **2016**, *51*, 591–602. [[CrossRef](#)]
29. Mathur, R.; Munk, L.; Nguyen, M.; Gregory, M.; Annell, H.; Lang, J. Modern and paleofluid pathways revealed by Cu isotope compositions in surface waters and ores of the Pebble porphyry Cu-Au-Mo deposit, Alaska. *Econ. Geol.* **2013**, *108*, 529–541. [[CrossRef](#)]
30. Chen, H.Q.; Qu, X.M.; Fan, S.F. Geological characteristics and metallogenic prospecting model of Duolong porphyry copper gold ore concentration area in Gerze County, Tibet. *Miner. Depos.* **2015**, *34*, 321–332.

31. Song, Y.; Yang, H.H.; Lin, B.; Liu, Z.B.; Qin, W.; Ke, G.; Chao, Y.; Xiang, F. The Preservation System of Epithermal Deposits in South Qiangtang Terrane of Central Tibetan Plateau and Its Significance: A Case Study of the Tiegelongnan Superlarge Deposit. *Acta Geosci. Sin.* **2017**, *38*, 659–669. (In Chinese)
32. Kapp, P.; Yin, A.; Manning, C.; Harrison, T.; Taylor, M.; Ding, L. Tectonic evolution of the early Mesozoic blueschist-bearing Qiangtang metamorphic belt, central Tibet. *Tectonics* **2003**, *22*. [[CrossRef](#)]
33. Kapp, P.; Yin, A.; Harrison, T.; Ding, L. Cretaceous-Tertiary shortening, basin development, and volcanism in central Tibet. *Geol. Soc. Am. Bull.* **2005**, *117*, 865–878. [[CrossRef](#)]
34. Pullen, A.; Kapp, P.; Gehrels, G.; Ding, L.; Zhang, Q. Metamorphic rocks in central Tibet: Lateral variations and implications for crustal structure. *Geol. Soc. Am. Bull.* **2011**, *123*, 585–600. [[CrossRef](#)]
35. Liu, D.; Huang, Q.; Fan, S.; Zhang, L.; Shi, R.; Ding, L. Subduction of the Bangong–Nujiang Ocean: Constraints from granites in the Bangong Co area, Tibet. *Geol. J.* **2014**, *49*, 188–206. [[CrossRef](#)]
36. Hao, L.; Wang, Q.; Wyman, D.A.; Ou, Q.; Dan, W.; Jiang, Z.; Wu, F.; Yang, J.; Long, X.; Li, J. Underplating of basaltic magmas and crustal growth in a continental arc: Evidence from Late Mesozoic intermediate-felsic intrusive rocks in southern Qiangtang, central Tibet. *Lithos* **2016**, *245*, 223–242. [[CrossRef](#)]
37. Zhu, D.; Li, S.; Cawood, P.; Wang, Q.; Zhao, Z.; Liu, S.; Wang, L. Assembly of the Lhasa and Qiangtang terranes in central Tibet by divergent double subduction. *Lithos* **2016**, *245*, 7–17. [[CrossRef](#)]
38. Allmendinger, R.; Jordan, T.; And, S.; Isacks, B. The evolution of the Altiplano-Puna plateau of the Central Andes. *Annu. Rev. Earth Planet. Sci.* **1997**, *25*, 139–174. [[CrossRef](#)]
39. Zhu, D.; Pan, G.; Wang, L.; Mo, X.; Zhao, Z.; Zhou, C.; Liao, Z.; Dong, G.; Yuan, S. Tempo-spatial variations of Mesozoic magmatic rocks in the Gangdese belt, Tibet, China, with a discussion of geodynamic setting-related issues. *Geol. Bull. China* **2008**, *27*, 1535–1550. (In Chinese)
40. Kapp, P.; Decelles, P.; Gehrels, G.; Heizler, M.; Lin, D. Geological records of the Lhasa-Qiangtang and Indo-Asian collisions in the Nima area of central Tibet. *Geol. Soc. Am. Bull.* **2007**, *119*, 917–933. [[CrossRef](#)]
41. Yin, A.; Harrison, T.M. Geologic evolution of the Himalayan-Tibetan orogen. *Annu. Rev. Earth Planet. Sci.* **2000**, *28*, 211–280. [[CrossRef](#)]
42. Qu, X.-M.; Wang, R.; Xin, H.; Jiang, J.; Chen, H. Age and petrogenesis of A-type granites in the middle segment of the Bangonghu–Nujiang suture, Tibetan plateau. *Lithos* **2012**, *146*, 264–275. [[CrossRef](#)]
43. Li, J.-X.; Qin, K.; Li, G.; Xiao, B.; Zhao, J.; Cao, M.; Chen, L. Petrogenesis of ore-bearing porphyries from the Duolong porphyry Cu–Au deposit, central Tibet: Evidence from U–Pb geochronology, petrochemistry and Sr–Nd–Hf–O isotope characteristics. *Lithos* **2013**, *160*, 216–227. [[CrossRef](#)]
44. Li, X.; Li, C.; Sun, Z.; Wang, M. Origin and tectonic setting of the giant Duolong Cu–Au deposit, South Qiangtang Terrane, Tibet: Evidence from geochronology and geochemistry of Early Cretaceous intrusive rocks. *Ore Geol. Rev.* **2017**, *80*, 61–78. [[CrossRef](#)]
45. Li, G.; Qin, K.; Li, J.; Evans, N.; Zhao, J.; Cao, M.; Zhang, X. Cretaceous magmatism and metallogeny in the Bangong–Nujiang metallogenic belt, central Tibet: Evidence from petrogeochemistry, zircon U–Pb ages, and Hf–O isotopic compositions. *Gondwana Res.* **2017**, *41*, 110–127. [[CrossRef](#)]
46. Hou, Z.; Mo, X.; Gao, Y.; Qu, X.; Meng, X. Adakite, a possible host rock for porphyry copper deposits: Case studies of porphyry copper belts in Tibetan Plateau and in Northern Chile. *Miner. Depos.* **2003**, *22*, 1–12. (In Chinese)
47. Defant, M.J.; Drummond, M.S. Derivation of some modern arc magmas by melting of young subducted lithosphere. *Nature* **1990**, *347*, 662. [[CrossRef](#)]
48. Sillitoe, R. Epochs of intrusion-related copper mineralization in the Andes. *J. S. Am. Earth Sci.* **1988**, *1*, 89–108. [[CrossRef](#)]
49. Sillitoe, R.H. A plate tectonic model for the origin of porphyry copper deposits. *Econ. Geol.* **1972**, *67*, 184–197. [[CrossRef](#)]
50. Hou, Z.; Gao, Y.; Qu, X.; Rui, Z.; Mo, X. Origin of adakitic intrusives generated during mid-Miocene east–west extension in southern Tibet. *Earth Planet. Sci. Lett.* **2004**, *220*, 139–155. [[CrossRef](#)]
51. Hou, Z.; Yang, Z.; Lu, Y.; Kemp, A.; Zheng, Y.; Li, Q.; Tang, J.; Yang, Z.; Duan, L. A genetic linkage between subduction-and collision-related porphyry Cu deposits in continental collision zones. *Geology* **2015**, *43*, 247–250. [[CrossRef](#)]

52. Oyarzun, R.; Márquez, A.; Lillo, J.; López, I.; Rivera, S. Reply to Discussion on “Giant versus small porphyry copper deposits of Cenozoic age in northern Chile: Adakitic versus normal calc-alkaline magmatism” by Oyarzun R, Márquez A, Lillo J, López I, Rivera S (Mineralium Deposita 36: 794–798, 2001). *Miner. Depos.* **2002**, *37*, 795–799. [[CrossRef](#)]
53. Li, J.; Qin, K.; Li, G.; Richards, J.; Zhao, J.; Cao, M. Geochronology, geochemistry, and zircon Hf isotopic compositions of Mesozoic intermediate-felsic intrusions in central Tibet: Petrogenetic and tectonic implications. *Lithos* **2014**, *198–199*, 77–91. [[CrossRef](#)]
54. Lv, L.; Zhao, Y.; Song, L.; Tian, Y.; Xin, H. Characteristics of C, Si, O, S and Pb isotopes of the Fe-rich and Cu (Au) deposits in the western Bangong–Nujiang metallogenic belt, Tibet, and their geological significance. *Acta Geol. Sin.* **2011**, *85*, 1291–1304. (In Chinese)
55. Xin, H.; Qu, X.; Wang, R.; Liu, H.; Zhao, Y.; Wei, H. Geochemistry and Pb, Sr, Nd isotopic features of ore-bearing porphyries in Bangong Lake porphyry copper belt, western Tibet. *Miner. Depos.* **2009**, *28*, 785–792. (In Chinese)
56. Hawkesworth, C. The generation and evolution of the continental crust. *J. Geol. Soc.* **2010**, *167*, 229–248. [[CrossRef](#)]
57. Richards, J.P. Postsubduction porphyry Cu-Au and epithermal Au deposits: Products of remelting of subduction-modified lithosphere. *Geology* **2009**, *37*, 247–250. [[CrossRef](#)]
58. Sillitoe, R. Styles of high-sulphidation gold, silver and copper mineralisation in porphyry and epithermal environments. In Proceedings of the Australasian Institute of Mining and Metallurgy, Melbourne, Australia, 11–13 September 2000; Volume 305, pp. 19–34.
59. Fournier, R.O. Hydrothermal processes related to movement of fluid from plastic into brittle rock in the magmatic-epithermal environment. *Econ. Geol.* **1999**, *94*, 1193–1211. [[CrossRef](#)]
60. Zhang, K.; Zhang, Y.; Tang, X.; Xia, B. Late Mesozoic tectonic evolution and growth of the Tibetan plateau prior to the Indo-Asian collision. *Earth Sci. Rev.* **2012**, *114*, 236–249. [[CrossRef](#)]
61. Li, Y.; Wang, C.; Li, Y.; Ma, C.; Wang, L.; Peng, S. The Cretaceous tectonic event in the Qiangtang Basin and its implications for hydrocarbon accumulation. *Pet. Sci.* **2010**, *7*, 466–471. [[CrossRef](#)]
62. Yang, K.; Ma, C. Some advances in the rates of continental erosion and mountain uplift. *Geol. Sci. Technol. Inf.* **1996**, *15*, 89–96.
63. Kesler, S.E.; Wilkinson, B.H. The role of exhumation in the temporal distribution of ore deposits. *Econ. Geol.* **2006**, *101*, 919–922. [[CrossRef](#)]
64. Murphy, M.; Yin, A.; Harrison, T.; Dürr, S.; Chen, Z.; Ryerson, J.; Kidd, F.; Wang, X.; Zhou, X. Did the Indo-Asian collision alone create the Tibetan plateau? *Geology* **1997**, *25*, 719–722. [[CrossRef](#)]
65. Ketcham, R.A. Forward and inverse modeling of low-temperature thermochronometry data. *Rev. Mineral. Geochem.* **2005**, *58*, 275–314. [[CrossRef](#)]
66. Yang, H.H.; Tang, J.; Dilles, J.; Song, Y. Temperature Study of the Duolong Porphyry Cu-Au District and its implications for the Evolution of the Qiangtang Terrane in Tibet, China. *Int. Geol. Rev.* **2018**. submitted.
67. Li, G. High temperature, salinity and strong oxidation ore-forming fluid at Duobuza gold-rich porphyry copper in the Bangonghu tectonic belt, Tibet: Evidence from fluid inclusions study. *Acta Petrol. Sin.* **2007**, *23*, 935–952.
68. Sillitoe, R.H. Porphyry Copper Systems. *Econ. Geol.* **2010**, *105*, 3–41. [[CrossRef](#)]
69. Lowell, J.D.; Guilbert, J.M. Lateral and vertical alteration-mineralization zoning in porphyry ore deposits. *Econ. Geol.* **1970**, *65*, 373–408. [[CrossRef](#)]



© 2018 by the authors. Licensee MDPI, Basel, Switzerland. This article is an open access article distributed under the terms and conditions of the Creative Commons Attribution (CC BY) license (<http://creativecommons.org/licenses/by/4.0/>).